Journal of Chromatography, 237 (1982) 185–198
Elsevier Scientific Publishing Company, Amsterdam — Printed in The Netherlands

CHROM. 14,468

PROTEIN–PROTEIN INTERACTIONS STUDIED BY COUNTER-CURRENT DISTRIBUTION

III. SIMULATION OF SELF-ASSOCIATING SYSTEMS

LARS BACKMAN
Department of Biochemistry, University of Umeå, S-901 87 Umeå (Sweden)
(Received October 22nd, 1981)

SUMMARY

Biological macromolecules that undergo self-association in solution are widely encountered. As differences in surface properties, such as charge and hydrophobicity, between monomeric and polymeric forms, are very probable it should be possible to use the counter-current distribution technique in two-phase liquid systems for the study of self-association.

The distribution behaviour of a self-associating solute has been simulated in order to establish the boundary conditions and limitations as well as potentials of the counter-current distribution technique as a tool for studying self-associations. The distributions have been calculated for a range of association constants, partition coefficients and initial solute concentration as well as for small zone and moving boundary counter-current distribution.

INTRODUCTION

Self-association of biological macromolecules in solution is a widely encountered phenomenon. The degree of self-association is usually dependent on solution conditions such as pH, ionic strength and temperature.

A self-association can be represented by equilibria of the type

$$j\,P_1 \rightleftharpoons P_j \qquad j = 2, 3, \ldots \tag{1}$$

or

$$j\,P_1 \rightleftharpoons r\,P_m + s\,P_n \tag{2}$$

and related equilibria, where P represents the self-associating solute.

In principle, self-associations can be studied by almost any experimental method that can differentiate between monomer and polymer(s) in some respect, *e.g.*, molecular weights or surface properties. However, sedimentation velocity and

0021-9673/82/0000–0000/$02.75

equilibrium, elastic light scattering, membrane osmometry and molecular sieve chromatography are the most extensively used techniques[1]. Many other methods, such as various spectroscopic techniques, calorimetry and isoelectric focusing, have been described and used for the analysis of associating systems[1]. Single-step partitions[2–4] and counter-current distribution (CCD)[5–7] in aqueous two-phase systems have been used successfully to study heterogeneous protein–protein interactions. Therefore, both partitions and CCD should also be suitable for the analysis of self-associations. In fact, the tetramer–dimer dissociation of human oxy- and methaemoglobin has been studied by Middaugh and Lawson using single-step partitions[8]. The CCD behaviour of self-associating solutes has also been predicted from the concentration dependence of the partition coefficients of the solutes[9]. However, to my knowledge the CCD method has not been used to analyse macromolecular self-associations.

In order to establish boundary conditions and limitations as well as possibilities of the CCD method as a tool for the study self-associations it was necessary to make a thorough theoretical investigation of the method. Therefore, the dependence of the CCD behaviour of monomer–*j*-mer and monomer–*m*-mer–*n*-mer equilibria on association constants, partition coefficients and initial solute concentration was studied. Monomer–single polymer equilibria in small zone CCD have previously been treated theoretically although incompletely by Bethune and Kegeles[10]. However, their approach is not useful for the description and future adaptation to experiments in aqueous two-phase systems owing to the unrealistic values assigned to the partition coefficients and the initial mass of the solute. On the other hand, the theoretical treatments of moving boundary CCD[11,12] are much more extensive. However, these treatments are not primarily aimed at the description of CCD behaviour but rather to incorporate diffusional effects in continuous transport systems, *i.e.*, sedimentation velocity.

In this paper, the behaviour of equilibria of types 1 and 2 in small zone CCD and moving boundary CCD are discussed.

CALCULATIONS

In the following description of the equilibration of a self-associating system between two phases it is assumed that the two phases are immiscible, that no volume change occurs upon mixing and equilibration, that all solutions are thermodynamically ideal and that there is equilibrium both within and between the phases before a transfer. Further, the total concentration of solute in any chamber is expressed as total monomer concentration.

If a monomer–*j*-mer association occurs in such a biphasic system, then the various equilibria would be

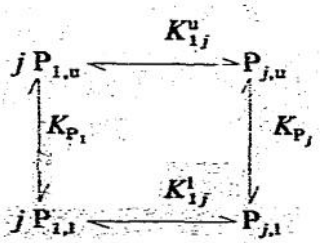

(3)

where the subscripts u and l refer to the upper and lower phase, respectively. The equilibria within each phase are described by the association constants, K^{u}_{1j} and K^{l}_{1j}, defined as

$$K^{x}_{1j} = \frac{[P_j]_x}{([P_1]_x)^j} \tag{4}$$

where x = u or l and the square brackets denote concentrations in moles per litre. The partition coefficient of each solute, i.e., K_{P_1} and K_{P_j}, defined as

$$K_{P_z} = \frac{[P_z]_u}{[P_z]_l} \tag{5}$$

where $z = 1$ or j, represent the equilibrium between the two phases.

Similarly, self-associations of type 2 can be depicted by

$$\begin{array}{ccccc} j\,P_{1,u} & \xrightarrow{K^{u}_{1mn}} & r\,P_{m,u} & + & s\,P_{n,u} \\ \uparrow K_{P_1} & & \uparrow K_{P_m} & & \uparrow K_{P_n} \\ j\,P_{1,l} & \xrightarrow{K^{l}_{1mn}} & r\,P_{m,l} & + & s\,P_{n,l} \end{array} \tag{6}$$

where

$$K^{x}_{1mn} = \frac{([P_m]_x)^r\ ([P_n]_x)^s}{([P_1]_x)^j} \tag{7}$$

where x = u or l. However, the formation of higher polymeric species can be considered to occur in a single-step association or through step-wise associations. In the former case the concentration of any polymeric form can be expressed by equations such as eqn. 4. In the latter case the concentration of any polymeric form is given by

$$[P_m] = [P_1]^m \prod_{\substack{g=0 \\ h=g+1}}^{m-1} K_{gh} \tag{8}$$

where, by definition, $K_{01} = 1$. The subsequent equations are developed in the same manner as previously[13] for repeated partitions, CCD, in which the lower phase is held stationary and the upper phase is transferred after equilibrium to the next chamber in sequence.

The total concentration of solute, expressed as monomeric concentration, in the ith chamber after n transfers is obtained by summation of all species in solution at equilibrium

$$[P_1]^{in}_{tot} = \sum_j (p\,j\,[P_j]^{in}_u + q\,j\,[P_j]^{in}_l) \tag{9}$$

where p and q are the fractions of volume of the upper and the lower phase, respectively. Eqn. 9 can be rewritten by inserting eqns. 4, 5 and 8 as

$$[P_1]_{tot}^{in} = \sum_j j\,([P_1]_l^{in})^j\,\alpha_j \tag{10}$$

where

$$\alpha_j = (p\,K_{P_j} + q)\,K_{1j}^1 \tag{11}$$

or

$$\alpha_j = (p\,K_{P_j} + q) \prod_{\substack{g=0 \\ h=g+1}}^{j-1} K_{gh}^1 \tag{12}$$

depending on the type of self-association.

Small zone CCD

In a small zone CCD experiment the solute is initially introduced into the first m chambers. Thus, the total concentration in these chambers before the first transfer are

$$[P_1]_{tot}^{x0} = \sum_j (p\,j\,[P_j]_u^{x0} + q\,j\,[P_j]_l^{x0}) \tag{13}$$

where $x = 0, 1, \ldots, m$. Given the initial values of total concentration and assigning values to the association constant(s) in the lower phase (or in the upper phase) and to the partition coefficients, the equilibrium concentration of the monomer in each lower phase can be determined. From these values the other equilibrium concentrations in each chamber can be calculated. Each upper phase is then transferred to the next chamber in sequence, except that the upper phase of the last chamber, *i.e.*, chamber n, is transferred to chamber zero. The first transfer is accomplished by calculating the total concentrations in chambers zero to $m + 1$ after the transfer using

$$[P_1]_{tot}^{01} = \sum_j (p\,j\,[P_j]_u^{n0}) + \sum_j (q\,j\,[P_j]_l^{00}) \tag{14}$$

$$[P_1]_{tot}^{x1} = \sum_j (p\,j\,[P_j]_u^{x-10}) + \sum_j (q\,j\,[P_j]_l^{x0}) \tag{15}$$

where $x = 1, 2, \ldots, m + 1$. Eqn. 10 is then solved for $m + 1$ chambers using the new values of total concentrations, yielding $m + 1$ sets of equilibrium concentrations for these chambers. Hence, by repeating this process, the final CCD pattern is obtained for n transfers.

Moving boundary CCD

In a moving boundary CCD experiment a plateau of original concentration

must be maintained throughout the experiment. A plateau is obtained if the number of chambers initially containing the solute is greater than the number of transfers, *i.e.*, $m > n$, and chamber zero is fed with pure upper phase at each transfer.

The equilibrium concentrations before a transfer and the total concentrations after a transfer in each chamber are obtained in the same manner as in small zone CCD. However, the total concentration in chamber zero after n transfers is given by

$$[P_1]_{tot}^{0n} = \sum_j (q\, j\, [P_j]_l^{0n-1}) \tag{16}$$

where $n = 1, 2, \ldots, n$. Correspondingly, the complete moving boundary CCD pattern is obtained by repetition of this process.

The programs, written in Basic for a Hewlett-Packard 9835 desk-top computer and in Fortran for a Cyber 172 computer, were mainly checked by summation of the equilibrium concentrations in all chambers after each transfer. The total amount of solute in all chambers never differed from that initially introduced by more than 1 part in 10^8.

The programs were also checked by letting all partition coefficients be equal or by setting the association constants equal to zero. In both instances the simulated CCD patterns should coincide with appropriate binomial curves, which they also did.

RESULTS AND DISCUSSION

After the completion of a CCD experiment all the extractable information, *e.g.*, pattern position, partition coefficients, homogeneity and distribution behaviour, are concealed in the resulting CCD pattern. Part of this information can be enhanced by taking the first derivative of the pattern. The first derivative or concentration gradient is particularly useful for detecting abnormalities in the distribution behaviour. Thus, the gradient should also be useful for comparing the CCD behaviour of different self-associating systems.

As CCD is a discontinuous process, the concentration gradient must be approximated by taking the differences between solute concentrations in adjacent chambers. Further, for the sake of clarity only the part of the concentration gradient patterns corresponding to the dispersed edges of the CCD patterns have been plotted in the figures.

The CCD pattern of a reversible self-associating solute is dependent on the initial concentration and the association constants as well as on the partition coefficients and the number of transfers. If the polymers migrate more rapidly than the monomer, *i.e.*, $KP_1 < KP_2, KP_3, \ldots$, then the polymeric species in the forward edge of the zone will migrate into chambers of low solute concentration. The equilibrium is thus shifted towards dissociation of polymers to form more slowly migrating monomers. Consequently, a hyper-sharpened boundary is formed at the forward edge, whereas at the backward edge the boundary is extended as dilution by polymer migration continually shifts the solute composition to a higher monomer content. This is analogous to the behaviour of a self-associating solute in molecular sieve chromatography[14,15]. The effects on the boundaries would obviously be reversed if the partition coefficient of the monomer is greater than those of the polymers, as demonstrated in Fig. 1.

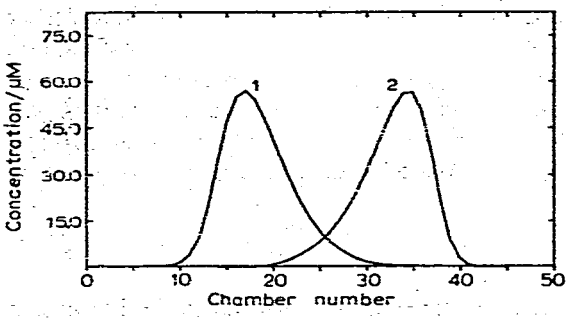

Fig. 1. Influence of the partition coefficients on the CCD behaviour of a monomer–dimer–trimer association. The initial solute concentration was 0.5 mM, the number of transfers was 50 and the association constants in the lower phase, K^l_{12} and K^l_{23}, were both $1 \cdot 10^4$ M^{-1}. The partition coefficients of monomer, dimer and trimer were 0.8, 0.5 and 0.2 (curve 1) and 1.25, 2 and 5 (curve 2), respectively.

As the migration continues the solute spreads into an increasing number of chambers and the relative monomer content of the solute is thereby gradually increased. Accordingly, as the number of transfers increases, the migration rate of the zone slowly approaches that of the monomer but nevertheless the hyper-sharpening and the dispersion of the boundaries persist, as Fig. 2 illustrates.

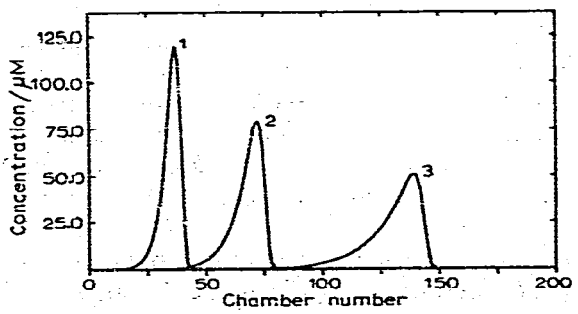

Fig. 2. Influence of the number of transfers on the CCD behaviour of a monomer–dimer association. The initial solute concentration was 1 mM, the association constant in the lower phase was 5000 M^{-1} and the partition coefficients of monomer and dimer were 1 and 5, respectively. The number of transfers was 50 (curve 1), 100 (curve 2) and 200 (curve 3).

The solute composition in any chamber is determined by the total solute concentration in that chamber and by the association constants, whereas the position of the zone is also determined by the partition coefficients. Therefore, the value of the association constants and the initial solute concentration determine the ratio of monomer to polymer and thus the degree of hyper-sharpening and dispersion of the CCD pattern.

Small zone CCD

The CCD behaviour of a series of self-associating systems was simulated and some typical results are shown in Figs. 3–7. The different CCD patterns represent different assignments to the values of the relevant association constants, and the

values for each class were chosen to cover a range from relatively loose to relatively tight association.

Monomer–dimer systems

Fig. 3a shows the CCD patterns produced by simulating the counter-current distribution of a monomer–dimer associating system. For a sufficiently loose association the solute zone migrates at the same rate as the monomer and, hence, the resulting CCD pattern is indistinguishable from a binomial one calculated with the partition coefficient of the monomer. The migration rate of the solute zone will approach that of the dimer as the association constants are increased and the dimer content thus becomes significant. Finally, at infinite association the migration rate will be the same as that of the dimer. Similar behaviour can be observed if the initial solute concentration is varied instead of the association constants. The corresponding concentration gradient patterns are shown in Fig. 3b. The patterns are unimodal and smooth; none of them shows any shoulder or inflection. Further, in all of the calculated gradient patterns the parts corresponding to the dispersed edge of the CCD pattern are appreciably skewed in the same direction, and the degree of skewing increases as the association becomes tighter.

In a previous paper[13] we postulated that the model for heterogeneous 1:1 interactions could be used to simulate dimerization patterns. However, this conclusion has now been found to be incorrect.

Monomer–trimer systems

CCD patterns generated by the model using different values of the monomer–

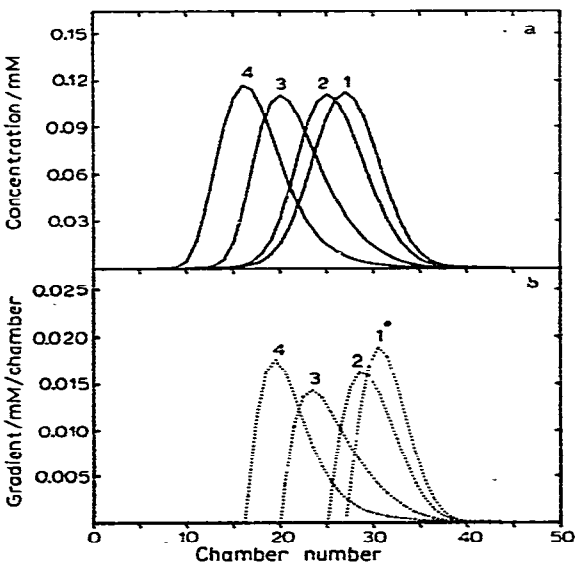

Fig. 3. (a) Simulated CCD patterns and (b) corresponding concentration gradient patterns of a monomer–dimer association. The initial solute concentration was 1 mM, the number of transfers was 50 and the partition coefficients of monomer and dimer were 1.2 and 0.4, respectively. The association constant in the lower phase was 100 M^{-1} (curve 1), 1000 M^{-1} (curve 2), $1 \cdot 10^4$ M^{-1} (curve 3) and $1 \cdot 10^5$ M^{-1} (curve 4).

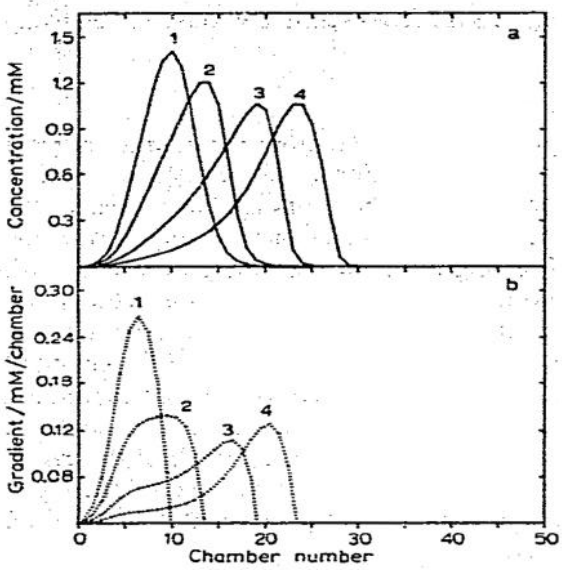

Fig. 4. (a) Simulated CCD patterns and (b) corresponding concentration gradient patterns of a monomer–trimer association. The initial solute concentration was 10 mM, the number of transfers was 50 and the partition coefficients of monomer and trimer were 0.2 and 1.5, respectively. The association constant in the lower phase was 1000 M^{-2} (curve 1), $1 \cdot 10^4$ M^{-2} (curve 2), $1 \cdot 10^5$ M^{-2} (curve 3) and $1 \cdot 10^6$ M^{-2} (curve 4).

trimer association are shown in Fig. 4a. The patterns are very similar to those simulated for a monomer–dimer system; the hyper-sharpening and dispersion progressively increase as the association becomes tighter or the initial concentration increases.

A useful diagnostic according to Bethune and Kegeles[10] for distinguishing between monomer–dimer and monomer–trimer associations in CCD should be the presence of an additional inflection point on the dispersed edge in the latter case. Hence, there should be a third optimum in the concentration gradient pattern.

The gradient patterns in Fig. 4b do not fulfil the predictions of the model of Bethune and Kegeles[10]. Only in gradient patterns 3 and 4 is a tendency to develop an extra optimum clearly apparent. In the part of pattern 2 corresponding to the dispersed edge no shoulder or inflection is visible; the main feature is its strange broadened shape. However, if the values assigned to the partition coefficients are extreme, *e.g.*, $KP_1 = 15$ and $KP_3 = 0.15$, the additional inflection in the CCD pattern will be visible. A similar discrepancy is also found between the asymptotic and diffusion models of sedimentation velocity[16] and molecular sieve chromatography[17].

Monomer–tetramer and monomer–hexamer systems

The simulated CCD patterns of monomer–tetramer associations (Fig. 5a) differ substantially from those patterns obtained for monomer–trimer and monomer–dimer associations. The patterns are not as smooth as before and the additional inflection point is readily apparent in patterns 3–5.

The concentration gradient patterns in Fig. 5b show a corresponding appearance. Patterns 3–5 exhibit distinct minima while pattern 2 shows a very marked shoulder. In pattern 1, for the weakest association, only an indication of a shoulder is

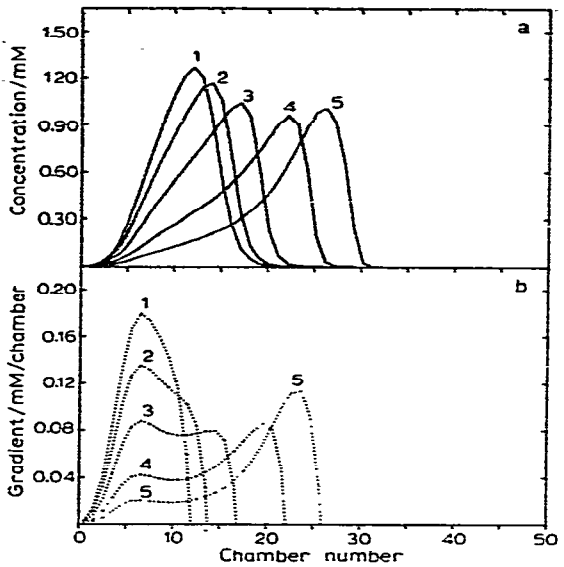

Fig. 5. (a) Simulated CCD patterns and (b) corresponding concentration gradient patterns of a monomer–tetramer association. The initial solute concentration was 10 mM, the number of transfers was 50 and the partition coefficients of monomer and tetramer were 0.2 and 1.5, respectively. The association constant in the lower phase was $1 \cdot 10^6\ M^{-3}$ (curve 1), $2.5 \cdot 10^6\ M^{-3}$ (curve 2), $1 \cdot 10^7\ M^{-3}$ (curve 3), $1 \cdot 10^8\ M^{-3}$ (curve 4) and $1 \cdot 10^9\ M^{-3}$ (curve 5).

evident. The most striking feature of the simulated gradient patterns for monomer–tetramer associations is, however, that all of the first maxima of the various gradient patterns lie nearly at the same position and, further, are very close to the position of the maximum for the monomer.

The effect of varying the association strength for a hexamerizing system resembles that of a tetramerizing system, as can be seen in Fig. 6. However, the presence of an inflection point on the dispersed edge of the CCD patterns is much more obvious. In this instance not only the first maxima but also the minima of the gradient patterns all lie at nearly the same position.

Monomer–dimer–trimer and related systems

These types of systems are much more complex than the other systems, because there are nearly no restrictions on the experimentally possible values of the partition coefficients. Hence there is no relationship between partition coefficient and size of the polymer as there is in molecular sieve chromatography[15].

The earlier approaches[11,12] of letting the velocities and the diffusion coefficients impose on the attainable values of the partition coefficients are not useful for a description of the distribution behaviour. Therefore, only a few simulations were made for these types of associations. Fig. 7 shows the resulting patterns for a monomer–dimer–trimer–tetramer system and for a monomer–dimer–tetramer system.

However, it is not possible to draw any general conclusion for the behaviour of these and related systems. The pattern can probably show any shape, depending on the values of the association constants and the partition coefficients.

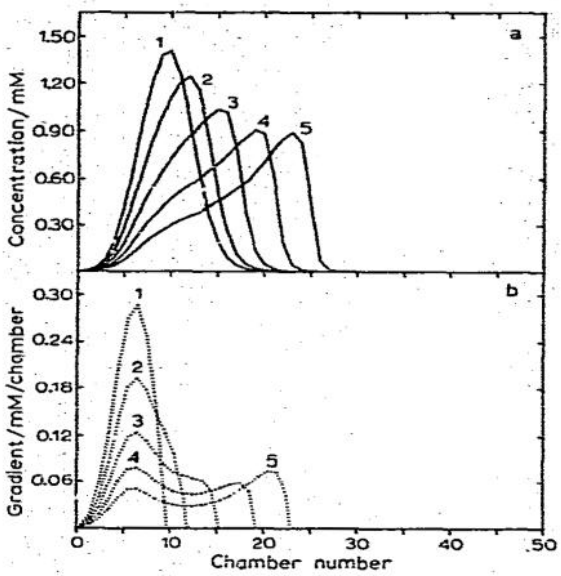

Fig. 6. (a) Simulated CCD patterns and (b) corresponding concentration gradient patterns of a monomer–hexamer association. The initial solute concentration was 10 mM, the number of transfers was 50 and the partition coefficients of monomer and hexamer were 0.2 and 1.5, respectively. The association constant in the lower phase was $1 \cdot 10^{10}$ M^{-5} (curve 1), $1 \cdot 10^{11}$ M^{-5} (curve 2), $1 \cdot 10^{12}$ M^{-5} (curve 3), $1 \cdot 10^{13}$ M^{-5} (curve 4) and $1 \cdot 10^{14}$ M^{-5} (curve 5).

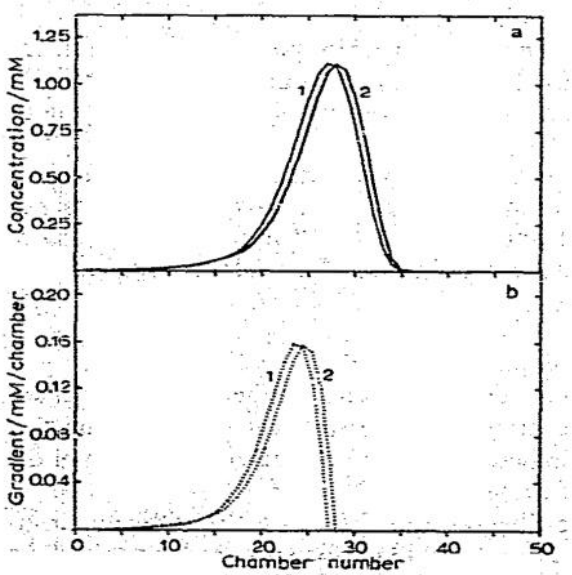

Fig. 7. (a) Simulated CCD patterns and (b) corresponding concentration gradient patterns of monomer–dimer–trimer–tetramer and monomer–dimer–tetramer associations. The initial solute concentration was 10 mM, the number of transfers was 50 and the partition coefficients of monomer, dimer, trimer and tetramer were 0.2, 0.7, 1.1 and 1.5, respectively. The association constants in the lower phase, K^l_{12}, K^l_{23} and K^l_{34}, describing the monomer–dimer–trimer–tetramer equilibrium were all $1 \cdot 10^4$ M^{-1} (curve 1). The association constants of the monomer–dimer–tetramer association, $K^l_{1,}$ and $K^l_{,4}$, were both $1 \cdot 10^4$ M^{-1} (curve 2).

Moving boundary CCD

In a moving boundary CCD experiment a plateau of constant solute concentration is created and maintained throughout the complete experiment. Therefore, as the solute zone migrates the forward and backward boundaries will be separated by a decreasing number of chambers of constant solute concentration equal to the initial solute concentration. In contrast, in a small zone experiment the initial plateau of solute concentration will not be sustained but will decrease progressively as the zone migrates and thus spreads in an increasing number of chambers. However, as the only substantial difference between small zone and moving boundary CCD is the maintenance of a plateau in the latter instance, the edges of the simulated moving boundary CCD patterns and the corresponding concentration gradient patterns must be very similar in shape to those generated by the small zone model. This is illustrated in Fig. 8, which shows the simulated moving boundary patterns for a monomer–tetramer system. Accordingly, the conclusions concerning small zone CCD are also valid for moving boundary CCD. Likewise, the typical features of the different types of self-associations are similar for both models. Further, the theory of moving boundary CCD of self-associating solutes has been treated fairly extensively previously, although not aimed towards the description of CCD[11,12]. Therefore, only one typical case of self-association is presented here, namely a monomer–tetramer system.

In Fig. 8a, it can be seen that the transformation of the dispersed edge of the CCD pattern as the binding becomes tighter closely resembles the transformation generated by the small zone model (Fig. 5a). Similarly, the concentration gradient

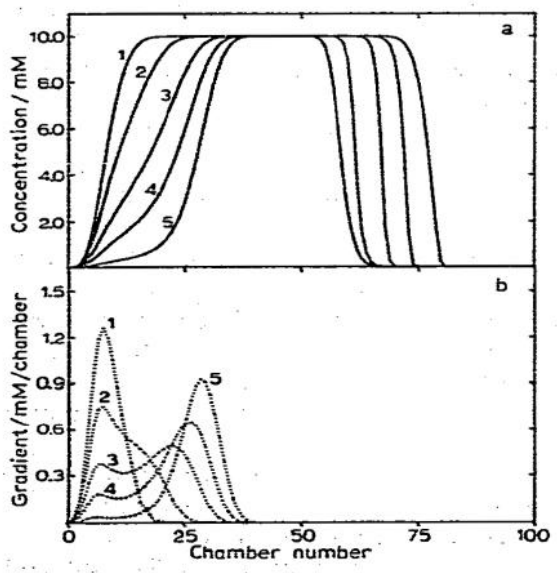

Fig. 8. (a) Simulated moving boundary CCD patterns and (b) corresponding concentration gradient patterns of a monomer–tetramer associations. The initial solute concentration in chambers 0–49 was 10 mM, the number of transfers was 50 and the partition coefficients of monomer and tetramer were 0.2 and 1.5, respectively. The association constant in the lower phase was 1000 M^{-3} (curve 1), $1 \cdot 10^4$ M^{-3} (curve 2), $1 \cdot 10^5$ M^{-3} (curve 3), $1 \cdot 10^6$ M^{-3} (curve 4) and $1 \cdot 10^8$ M^{-3} (curve 5).

patterns in Fig. 8b show the same appearance as before (Fig. 5b), from an indication of a shoulder to a distinct minimum depending on the binding strength.

For a certain degree or type of self-association, the shape of the patterns will depend on the partition coefficients, the association constants, the initial solute concentration and the number of transfers. Therefore, the simulations presented above should not be regarded as valid for all cases. It must be stressed that most of the simulations described here were obtained for one set of partition coefficients. If the difference in the values of the partition coefficients chosen were smaller, the typical features would be less preserved. On the other hand, if the difference between the partition coefficients were greater the characteristics of the patterns would be more pronounced.

Nevertheless, it seems possible to make some general comments on the basis of the calculations presented. Although both small zone and moving boundary CCD are discontinuous transport processes, they show the same general features as continuous transport processes such as sedimentation velocity[16,18] and molecular sieve chromatography[14,15,17,19]. It is reasonable to conclude that a solute self-associates whenever the distribution behaviour of the solute exhibits a concentration dependence. The converse conclusion, however, is not always correct. If the polymeric forms of the solute distribute similarly to the monomer in a particular two-phase system, obviously no hyper-sharpening or dispersion of the CCD pattern would be expected on formation of polymers. In such a case it should be possible to conclude whether the solute self-associates or not by changing the composition of the two-phase system, and thereby the partition of the different forms of the solute.

In a monomer–dimer equilibrium the dispersed edge of both the CCD and the gradient patterns must fall smoothly. Thence, a monomer–dimer association can be eliminated when a shoulder or a definite minimum is present in the experimental concentration gradient pattern. On the other hand, a monomer–trimer association will not necessarily generate a shoulder in the gradient pattern if the binding is relatively loose, as is evident in Fig. 4. The monomer–tetramer and monomer–hexamer cases studied display patterns that are easily distinguishable from monomer–trimer patterns, at least when the polymer content is significant. The additional inflection point is readily apparent and the gradient patterns show distinct minima. The position of the first maximum of the gradient pattern, if it appears, provides a useful diagnostic indicator. If the position is independent of the polymer content, *i.e.*, independent of the initial solute concentration or the binding strength, then monomer–dimer and monomer–trimer equilibria can be excluded. Further, the presence of tetrameric or hexameric species might be distinguished by the position of the minimum. However, these distinct features might not persist if other values of the partition coefficients are chosen.

From the appearance of the experimental CCD patterns and the corresponding concentration gradient patterns it is thus possible not only to detect a self-association but also, under certain circumstances, to determine the type of equilibrium.

Numerical analysis can, of course, be applied to experimental CCD results of self-associating solutes for quantifying the binding strength and partition coefficients of participating species. The method of least squares in connection with an iterative minimization procedure such as Simplex[20] has proved to be very useful for such purposes[8,21]. By generating patterns according to the different models by using the

known initial solute concentration and assigning values to the association constants and the partition coefficients, it is then possible to find a set of parameters that gives the best fitting simulated patterns for each model. The analysis procedure is thus capable of showing whether a particular model and set of parameters can account for the results of a CCD experiment.

Although the typical features of each model are similar for both small zone and moving boundary CCD, there are important distinctions between the two experimental procedures. The typical characteristics of each model are better preserved in moving boundary CCD, and the analysis of experimental CCD results becomes easier. In addition, the lower limit of the detectable binding strength becomes lower than for small zone CCD. However, the major disadvantage of moving boundary CCD is that large amounts of material are needed. Therefore, the choice between small zone CCD and moving boundary CCD is mainly dependent on the amount of material available and on the presumed binding strength.

The choice of two-phase system is not crucial for the theoretical considerations presented here. However, aqueous two-phase systems containing dextran and poly(ethylene glycol) have been shown to be very suitable for work with substances of biological origin[22]. The phases of these two-phase systems are rich in water and have a stabilizing effect on structure and biological activities. In particular, the partition coefficient can easily be adjusted by changing the composition of the two-phase system. Further, both dextran[23] and poly(ethylene glycol)[24,25] stimulate the association of proteins, probably owing to the excluded volume effect. It has been proposed[24,26] that polymers introduced into *in vitro* systems mimic the cell and would thereby provide a more normal cellular milieu than aqueous solutions of standard ionic strength and pH.

ACKNOWLEDGEMENT

I thank Dr. Vithaldas P. Shanbhag for valuable discussions and criticism.

REFERENCES

1 C. H. W. Hirs and S. N. Timasheff (Editors), *Methods in Enzymology*, Vol. 61, *Enzyme Structure* (Part H), and preceding volumes (Parts A–G), Academic Press, New York, 1979.
2 L. C. Petersen, *FEBS Lett.*, 94 (1978) 105–108.
3 J. S. Patton, P.-Å. Albertsson, C. Erlansson and B. Borgström, *J. Biol. Chem.*, 253 (1978) 4195–4202.
4 G. Fex, P.-Å. Albertsson and B. Hansson, *Eur. J. Biochem.*, 99 (1979) 353–360.
5 L. Backman and G. Johansson, *FEBS Lett.*, 65 (1976) 39–43.
6 D. N. Silverman, L. Backman and C. K. Tu, *J. Biol. Chem.*, 254 (1979) 2588–2591.
7 L. Backman, *Eur. J. Biochem.*, 120 (1981) 257–261.
8 C. R. Middaugh and E. Q. Lawson, *Anal. Biochem.*, 105 (1980) 364–368.
9 R. C. Williams, Jr. and L. C. Craig, *Sep. Sci.*, 2 (1967) 487–499.
10 J. L. Bethune and G. Kegeles, *J. Phys. Chem.*, 65 (1961) 433–438.
11 J. L. Bethune, *J. Phys. Chem.*, 74 (1970) 3837–3845.
12 B. J. McNeil, L. W. Nichol and J. L. Bethune, *J. Phys. Chem.*, 74 (1970) 3846–3852.
13 L. Backman and V. Shanbhag, *J. Chromatogr.*, 171 (1979) 1–13.
14 D. J. Winzor and H. A. Scheraga, *Biochemistry*, 2 (1963) 1263–1267.
15 G. K. Ackers, in H. Neurath and R. L. Hill (Editors), *The Proteins*, Vol. 1, Academic Press, New York, 3rd ed., 1975, pp. 1–94.
16 D. J. Cox, *Arch. Biochem. Biophys.*, 142 (1971) 514–526.

17 J. K. Zimmerman, D. J. Cox and G. K. Ackers, *J. Biol. Chem.*, 246 (1971) 4242–4250.
18 D. J. Cox, *Arch. Biochem. Biophys.*, 129 (1969) 106–123.
19 F. J. Stevens and M. Schiffer, *Biochem. J.*, 195 (1981) 213–219.
20 R. E. Ernst, *Rev. Sci. Instrum.*, 39 (1968) 998–1012.
21 L. Backman, *J. Chromatogr.*, 196 (1980) 207–216.
22 P.-Å. Albertsson, *Partition of Cell Particles and Macromolecules*, Almqvist and Wiksell, Stockholm, and Wiley, New York, 2nd ed., 1971.
23 T. C. Laurent, *Eur. J. Biochem.*, 21 (1971) 498–506.
24 L. W. Nichol, A. G. Ogston and P. R. Wills, *FEBS Lett.*, 126 (1981) 18–20.
25 L. A. Halper and P. A. Srere, *Arch. Biochem. Biophys.*, 184 (1977) 529–534.
26 P. A. Srere and J. G. Henslee, in L. Nover, F. Lynen and K. Mothes (Editors), *Cell Compartmentation and Metabolic Channeling*, VEB Gustav Fischer Verlag, Jena, and Elsevier/North-Holland Biomedical Press, Amsterdam, 1980, pp. 159–168.